BED1, a Gene Encoding a Galactosyltransferase Homologue, Is Required for Polarized Growth and Efficient Bud Emergence in *Saccharomyces cerevisiae*

Guillaume Mondésert and Steven I. Reed

Department of Molecular Biology, MB7, The Scripps Research Institute, La Jolla, California 92037

Abstract. The ellipsoidal shape of the yeast *Saccharomyces cerevisiae* is the result of successive isotropic/apical growth switches that are regulated in a cell cycle–dependent manner. It is thought that growth polarity is governed by the remodeling of the actin cytoskeleton that is itself under the control of the cell cycle machinery. The cell cycle and the morphogenesis cycle are tightly coupled and it has been recently suggested that a morphogenesis/polarity checkpoint control monitors bud emergence in order to maintain the coupling of these two events (Lew, D. J., and S. I. Reed. 1995. *J. Cell Biol.* 129:739–749). During a screen based on the inability of cells impaired in the budding process to survive when the morphogenesis checkpoint control is abolished, we identified and characterized *BED1*, a new gene that is required for efficient budding. Cells carrying a disrupted allele of *BED1* no longer have the wild-type ellipsoidal shape characteristic of *S. cerevisiae*, are larger than wild-type cells, are deficient in bud emergence, and depend upon an intact morphogenesis checkpoint control to survive. These cells show defects in polarized growth despite the fact that the actin cytoskeleton appears normal. Our results suggest that Bed1 is a type II membrane protein localized in the endoplasmic reticulum. *BED1* is significantly homologous to *gma12*$^+$, a *S. pombe* gene coding for an α-1,2-galactosyltransferase, suggesting that glycosylation of specific proteins or lipids could be important for signaling in the switch to polarized growth and in bud emergence.

THE ellipsoidal shape of the yeast *Saccharomyces cerevisiae* reflects cell cycle–regulated polarized growth. At specific times during the cell cycle, cell growth is either isotropic or polarized toward the bud (for review see Lew and Reed, 1995*b*). A correlation between local deposition of new cell wall components and actin localization has been established (Adams and Pringle, 1984; Kilmartin and Adams, 1984), leading to the proposal that actin directs secretory vesicles to specific regions of the plasma membrane to allow localized cell surface growth during bud initiation and bud growth. During most of the G1 phase, growth is isotropic and cortical actin patches are delocalized throughout the cell. The attainment of a critical cell size and concomitant execution of START lead to the formation of an actin ring at the pre-bud site and the orientation of actin filaments toward this site. Subsequent to START, growth is almost completely restricted to the emerging bud. During bud growth, cortical actin patches are localized to the bud. Initially, bud growth occurs primarily at the distal tip. At some point, though, there is a switch to isotropic growth first in the bud, then also transiently in the mother cell at mitosis. At cytokinesis, the actin cytoskeleton is reorganized and actin patches are relocalized to the mother-daughter neck where the cell wall is modified for cell separation. The mechanisms by which actin mediates polarized secretion are not well understood, but it has been shown that cortical actin patches are associated with the cell surface through an invagination of the plasma membrane (Mulholland et al., 1994) and it has been suggested that components of the secretory pathway (endoplasmic reticulum [ER] and Golgi) could be transported into the bud to direct localized growth presumably via an actin-dependent mechanism (Preuss et al., 1992).

A variety of proteins have been shown to be required for either bud emergence or for bud site selection (for recent reviews see Bretscher et al., 1994; Chant, 1994; Welch and Drubin, 1994). *CDC42*, encoding a small GTP-binding protein, and several genes encoding its regulators are involved in bud emergence: cells mutated in these genes arrest as large unbudded cells with a disorganized actin cytoskeleton and delocalized chitin. The *BUD* genes, along with *CDC24* and *RSV167* are involved in the selection of the bud site.

In *S. cerevisiae*, the budding cycle is tightly coupled to the central events of the cell cycle. Upon completion of the primary G1 restriction event known as START, when the

Address all correspondence to S. I. Reed, Department of Molecular Biology, MB7, The Scripps Research Institute, 10666 North Torrey Pines Road, La Jolla, California 92037. Tel.: (619)554-9836. Fax: (619)554-6188.

mother cell has reached a critical size, bud emergence and S phase are initiated (Nasmyth, 1993; Reed, 1992). Moreover, the dramatic changes of actin organization and the isotropic/apical growth switches observed during the cell cycle have been shown to be triggered by the different forms of the Cdc28 kinase that constitute the cell cycle clock (Lew and Reed, 1993). Furthermore, it has been recently suggested that growth polarity or bud emergence are monitored to ensure that mitosis does not occur before a bud is produced to receive the daughter nucleus (Lew and Reed, 1995*a*). The impairment of growth polarity either by mutation or external stimuli such as osmotic shock is detected and results in a G2 delay. This morphogenesis/polarity checkpoint control is mediated via a partial inhibition of transcription of the mitotic cyclin genes *CLB1* and *CLB2* and also through a more direct inhibition of the mitotic form of the Cdc28 kinase via negative regulatory phosphorylation of Tyr19 of Cdc28 (Lew and Reed, 1995*a*). This conserved tyrosine has been shown to be the target of negative regulatory phosphorylation for a number of different cyclin-dependent kinases.

In this paper, we describe the identification and the characterization of a new gene called *BED1* (which stands for Bud Emergence Delay)[1] that is required for efficient polarized growth and is important for bud emergence. The *bed1-1* mutation was isolated based on synthetic lethality with overexpression of mitotic cyclins, a phenotype that occurs because *bed1* mutant cells depend on the morphogenesis/polarity checkpoint which overexpression of mitotic cyclins overrides. We have shown that the Bed1 protein is an integral membrane protein localized in the endoplasmic reticulum. This protein shares homology with a previously described *S. pombe* α-1,2-galactosyltransferase. Our results suggest that glycosyl modification could play a role in regulating growth polarity and bud emergence.

1. *Abbrevations used in this paper*: BED, bud emergence delay; FOA, fluororotic acid; ORF, open reading frame.

Materials and Methods

Yeast Strains, Media, and Growth Conditions

All strains used in this study were derivatives of BF264-15DU: *MATa ade1, his2, leu2-3,112, trp1-1^a, ura3Dns* (Richardson et al., 1989). The relevant genotypes of strains used in this study are shown in Table I. Yeast cultures were grown at 30°C in YEP (1% yeast extract, 2% bactopeptone, 0.005% adenine, 0.005% uracil) supplemented with 2% glucose (YEPD), raffinose (YEPR), or galactose (YEPG). Genes under control of the *GAL1* promoter were induced by the addition of 2% galactose to a mid-log phase culture (YEPR) for 4 h.

Identification and Molecular Characterization of the BED1 Gene

A strain carrying a *GAL1:CLB2* allele (GY-1) was mutagenized by ultraviolet radiation (70% death) on YEPD plates (*GAL1* promoter repressed) and incubated at 30°C for 2 d. The colonies were then replica-plated to YEPG (*GAL1* promoter induced). Out of 25,000 colonies screened, 20 were unable to grow on galactose. Based on the level of Clb2 overexpression, we discarded 11 candidates that showed low levels of Clb2 protein after 4 h galactose induction of the *GAL:CLB2* allele, presumably because the mutations affected the galactose pathway. The nine remaining candidates were then crossed to the wild-type 15D strain and the resulting tetrads were analyzed to show that, for eight of them, the lethality was associated with overexpression of Clb2. The mutant strains were backcrossed to a *MATα-GAL1:CLB2* strain (GY-101) and the diploid strains were then induced to sporulate and meiotic asci dissected to verify that the lethality on YEPG was due to a single mutation and that the mutations were not localized to the *GAL1:CLB2* locus. A complementation analysis with the 8 remaining candidates showed that they belong to 6 different complementation groups, 2 of them with 2 alleles. We analyzed in greater detail one of them, that contains one allele, *bed1-1*.

The *BED1* gene was cloned by complementation of the lethality of the strain GY-159 (*GAL1:CLB2-bed1-1*) on YEPG plates with a YCp50 based genomic yeast DNA library (Rose et al., 1987). The screening of 15,000 transformants (the equivalent of 10 genomes) yielded the plasmid pR159.1 5 times and the plasmid pR159.5 a single time, containing inserts

Table I. Yeast Strains

Strain	Genotype	Source*
15Daub	MATa-ade1-his2-leu2-3,112-trp1-1*-ura3Dns-bar1Δ	S. I. R.
DLY-005	MATa/α	D. J. L.
GY-1	MATα-GAL1:CLB2(LEU2)	S. I. R.
GY-101	MATα-GAL1:CLB2(LEU2)	This study
GY-159	MATα-GAL1:CLB2(LEU2)-bed1-1	This study
GY-381	MATa-bed1::URA3	This study
GY-382	MATa-bed1::URA3-GAL1:CLB2(LEU2)	This study
GY-409C	MATα-bed1::URA3-GAL1:CLB2(LEU2)	This study
GY-449	MATa-bed1::URA3-cdc28::LEU2-cdc28^{F19A18}(TRP1)	This study
GY-488	MATα-bed1-1	This study
GY-489	MATα-bed1-1::BED1(LEU2)	This study
GY-647	MATa/α-bed1::URA3/bed1::ura3::LEU2	This study
GY-650	MATa/α-BED1/bed1-1::BED1(LEU2)	This study
GY-651	MATa/α-BED1::BED1(LEU2)/bed1-1	This study
GY-711	MATa-bed1::URA3-GAL1:BED1(LEU2)	This study
GY-713	MATa-bed1::URA3-GAL1:BED1[HA]3X(LEU2)	This study
GY-716	MATa-bed1::ura3::LEU2-GAP:BED1(URA3)	This study
GY-718	MATa-bed1::ura3::LEU2-GAP:BED1[HA]3X(URA3)	This study
GY-721	MATa-bed1::URA3-BED1(LEU2)	This study
GY-723	MATa-bed1::URA3-BED1[HA]3X(LEU2)	This study
GY-748	MATa-gal10Δ	This study
GY-755	MATa-BED1::BED1(LEU2)	This study

*S. I. R., Steven I. Reed; D. J. L., Daniel J. Lew.

of 12 kb and 9 kb, respectively (see Fig. 7 *A*). These two DNA fragments had an overlap α region of 2.7 kb that was able to rescue the lethality of the strain GY-159 on YEPG medium. This region was sequenced on both strands using an automated sequencing system (Applied Biosystems, Foster City, CA).

A diploid strain *BED1/bed1-1::BED1(LEU2)* (GY-650; see below) was constructed, induced to sporulate, and 48 tetrads were analyzed and 47 parental ditype (PD): 0 nonparental ditype (NPD): 1 tetratype (TT) were observed demonstrating a tight linkage between *bed1-1* and *LEU2* loci (~1 cM). We also created a diploid strain *BED1::BED1(LEU2)/bed1-1* (GY-651; see below), dissected 23 tetrads and 23 PD: 0 NPD: 0 TT were recovered, indicating again that the gene cloned by complementation was likely to correspond to the *BED1* locus defined mutationally.

Plasmids

The 2.7-kb DNA fragment defined by the region of overlap between plasmids pR159.1 and pR159.5 was subcloned into pBlueScript (Stratagene, La Jolla, CA) and the *BED1* gene was disrupted by replacing an 0.8-kb XbaI fragment within the coding region with a HindIII DNA fragment containing the *URA3* gene to give the plasmid pBS159::URA3C (see Fig. 1 *B*).

The *BED1* ORF was amplified by PCR using primers containing BamHI sites and a unique NotI site before the STOP codon (primers: 5′-CCC-C**GGATCC**ACAATATGTCTAGTGTACCT-3′; 5′-CCCC**GGATCC**TTA-GCGGCCGCCTGGGAAGAAAAATCTCGTGT-3′; the BamHI and NotI sites are indicated in bold characters and the ATG and STOP codons are underlined). The PCR product cloned into the pCRII vector (Invitrogen, San Diego, CA) and digested with BamHI was then cloned into the BamHI site of YIpG2 (LEU2) (Richardson et al., 1989), into the BglII site of pHV100(URA3) (a gift from H. Valdivieso), or into the BamHI site of YIpBED2(LEU2) to generate YIpG2:*BED1*, YIpGAP3:*BED1*, and YIpBED2:*BED1*, respectively. The YIpBED2(LEU2) vector contained a BglII–BamHI PCR fragment containing the promoter of the *BED1* gene (primers: 5′-CCCCAGATCTGAAGCAGGCTACTTATT-3′; 5′-CCCCGG-ATCCATAGTTGTACATGCACA-3′) cloned into the BamHI site of vector YIplac128 (Sikorski and Hieter, 1989). A NotI fragment containing three tandem copies of the HA epitope from the plasmid pGTEP1 (Tyers et al., 1992) was cloned into the NotI site of YIpG2:*BED1*, YIpGAP3:*BED1*, and YIpBED2:*BED1* to generate YIpG2:*BED1*[HA]3X, YIpGAP3:*BED1* [HA]3X and YIpBED2:*BED1*[HA]3X, respectively. The PCR products were sequenced to verify that no mutations were introduced during amplification.

Strain Construction

Strains were constructed according to standard genetic procedures (Sherman et al., 1982) except that transformations of yeast cells were performed as described by Elble (1992). The strain GY-381, disrupted for the *BED1* gene, was obtained by transformation of a wild-type haploid strain with the plasmid pBS159::URA3C digested with SstI. The disruption was verified by Southern analysis (not shown).

The *LEU2* marked *BED1* gene was inserted at the *bed1-1* locus by transformation of a *MATa-bed1-1* strain (GY-488) with the plasmid YIpBED2:*BED1* digested with NheI; this strain (GY-489) was then crossed to the 15Daub strain to create GY-650. The strain GY-651 was similarly obtained by insertion of the *LEU2* marked *BED1* allele at the *BED1* locus in 15Daub; this strain (GY-755) was then crossed to a *MATa-bed1-1* strain (GY-488). GY-650 and GY-651 were used to ascertain that the cloned *BED1* gene was mutated in the *bed1-1* strain.

The strains GY-711, GY-713, GY-721, and GY-723 were obtained by transformation of GY-381 with YIpG2:*BED1*, YIpG2:*BED1*[HA]3X, YIpBED2:*BED1*, and YIpBED2:*BED1*[HA]3X linearized within the *LEU2* marker with BstEII. The *URA3* marker in the *bed1* disruption was converted into a *LEU2* marker by inserting the *LEU2* marker into *URA3* with the plasmid pUL9 (a generous gift from Fred Cross) to generate the strain GY-582B. This strain was then transformed with YIpGAP3:*BED1* or YIpGAP3:*BED1*[HA]3X linearized in the *URA3* marker by EcoRV to give the strains GY-716 and GY-718, respectively.

The *GAL10* gene was disrupted by transplacement of a mutated version of gal10. The wild-type strain was transformed with the plasmid pBM58(URA3) (a generous gift from Mark Johnston) linearized with PvuII; gal$^-$ colonies were then recovered on 5-fluor-orotic acid (FOA) plates to select for transplacements.

Cell Biology Protocols

FACS analysis was performed on mid-log phase cultures as described previously (Lew et al., 1992).

Centrifugal elutriations were performed as previously described (Lew et al., 1992). Cells were grown to mid-log phase in YEPR medium and elutriated G1 cells from wild-type and mutant strains were inoculated into prewarmed YEPD medium at time 0 min. Aliquots were then taken every 15 min to analyze the following parameters: the timing of START was determined by incubating an aliquot of the culture at 30°C in the presence of α-factor (200 ng/ml, final concentration) for 45 min and the percentage of the cells that had passed START was determined by FACS analysis; the percentage of cells that had entered into S phase was estimated by FACS analysis; the budding index was evaluated by visually scoring a minimum of 200 cells; the timing of nuclear division was determined by counting the number of cells with two separated nuclei after staining with DAPI.

Nuclei were visualized with DAPI according to the following protocol: cells from mid-log phase cultures were fixed for 30 min in methanol:acetic acid (3:1) at room temperature, washed with 0.15 M NaCl, and stained for 30 min in the dark with 0.1 mg/ml DAPI.

Actin and chitin staining and in vivo labeling with FITC-ConA were performed as previously described (Adams and Pringle, 1991; Pringle, 1991; Lew and Reed, 1993).

Immunolocalization of the Bed1 HA-tagged protein was performed as previously described (Pringle et al., 1991) with the following modifications: cells from mid-log cultures were fixed with 3.7% formaldehyde added directly to the medium and incubated for 1 h at room temperature or overnight at 4°C; the cells were washed once with PBS and twice with 1 M Sorbitol/1 mM EDTA. The cell wall was then digested with Zymolyase (ICN Biochemicals, Costa Mesa, CA) in the presence of β-mercaptoethanol. Spheroplasts were washed twice with 1 M Sorbitol/1 mM EDTA, treated with 1% NP-40 for 5 min at room temperature and washed twice in 1 M Sorbitol/1 mM EDTA. Staining was performed on spheroplasts attached to poly-lysine–coated slides as previously described (Pringle et al., 1991) with the 12CA5 monoclonal antibody (Boehringer Mannheim Corp., Indianapolis, IN) at a concentration of 5 ng/ml. The secondary antibody was an FITC-conjugated goat serum directed against whole mouse IgG.

Protein Analysis

Protein extracts and cell fractionation were performed as described previously (Graham et al., 1994). Cells from mid-log phase cultures were spheroplasted with Zymolase and lysed to obtain total protein extracts with intact membrane structures. These extracts were then centrifuged for 15 min at 13,000 *g* to generate the P13 fraction and the supernatant was centrifuged at 100,000 *g* to obtain the P100 and the S100 fractions. The HA-tagged Bed1 fusion proteins were detected by Western blotting using the 12CA5 monoclonal antibody with the ECL detection kit (Amersham Corp., Arlington Heights, IL) as previously described (Grandin and Reed, 1993). Kar2 was detected with a rabbit serum kindly provided by M. Rose.

Results

Overexpression of the mitotic cyclins Clb1 or Clb2 under control of the *GAL1* promoter is not lethal in *S. cerevisiae*. The cells are only delayed in mitosis, presumably because the mitotic cyclin destruction pathway is sufficient to overcome the resultant elevated cyclin levels (Stueland et al., 1993; Amon et al., 1994), thus avoiding deleterious effects to the cell. We took advantage of these observations to implement a screen for mutants unable to tolerate high levels of Clb2 expression (see Materials and Methods). Cells carrying an inducible *CLB2* allele under the control of the *GAL1* promoter (GY-1) were mutagenized by UV irradiation and we selected mutants that were unable to grow on YEPG which induces the *GAL1:CLB2* allele. Two categories of mutations are expected from such a screen. First, cells affected in their ability to degrade mitotic cyclins will arrest in mitosis because they cannot overcome the accumulation of *CLB2* leading to chronic activation of the mi-

totic form of Cdc28 kinase. This situation would be analogous to the lethality observed when a nondegradable form of Clb1 (Clb1Δ152) is overexpressed in wild-type cells (Ghiara et al., 1991). A second expected class of mutation conferring a defect in bud emergence or growth polarity can also be obtained with this screening method. Delays or blocks in generation of growth polarity or in bud emergence are detected by a morphogenesis checkpoint leading to a temporary G2 arrest (Lew and Reed, 1995*a*). This control can be overridden either by mutation of tyrosine 19 of the Cdc28 kinase or the overexpression of mitotic cyclins Clb1 or Clb2 (Lew and Reed, 1995*a*). Therefore mutations that delay budding or the generation of growth polarity could confer a lethal phenotype when *CLB2* is overexpressed due to abrogation of the checkpoint. In this situation, cells dependent on the checkpoint would die with more than one nucleus as a result of mitosis occurring

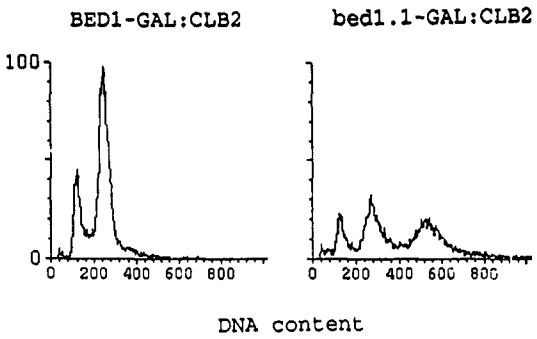

Figure 1. Overexpression of the mitotic cyclin Clb2 is lethal in a *bed1-1* background. The FACS profiles of *BED1GAL1:CLB2* (GY-1) and *bed1-1-GAL1:CLB2* (GY-159) strains were determined after 4 h induction with galactose.

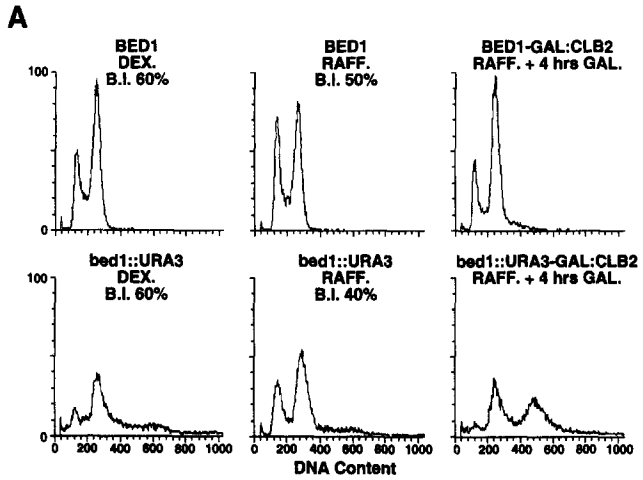

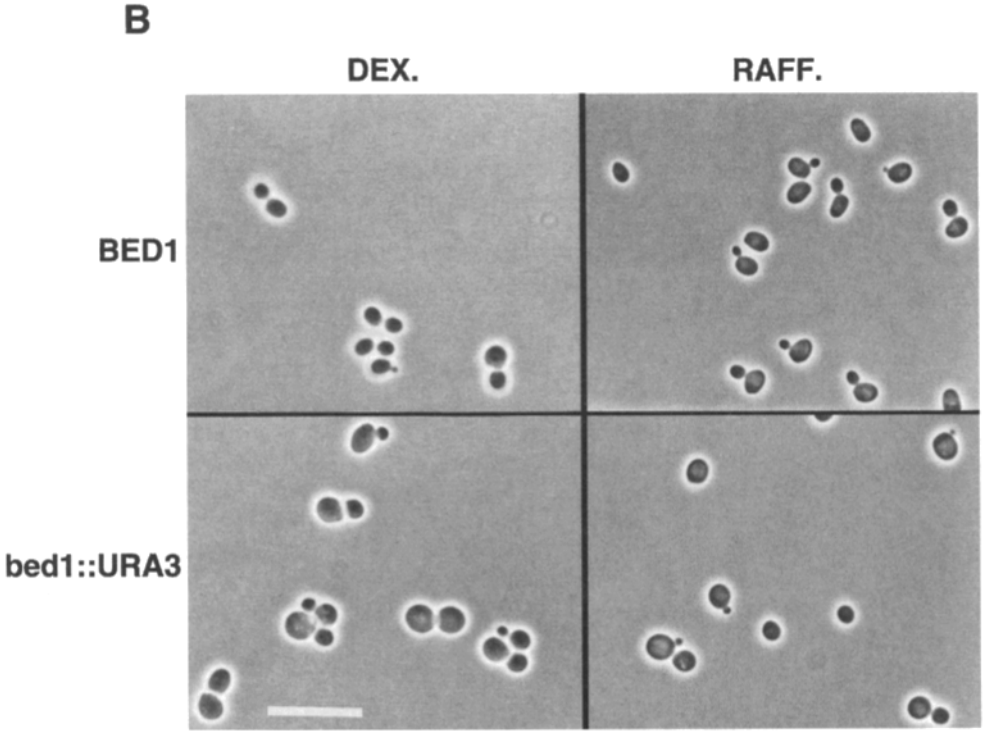

Figure 2. Phenotype *bed1* disruptant cells. (*A*) FACS analysis of *bed1::URA3* cells. Wild-type (15 Daub), *bed1::URA3* (GY-381) grown at mid-log phase in YEPD or YEPR, *BED1-GAL1::CLB2* (GY-1) and *bed1::URA3-GAL1:CLB2* (GY-382) induced at mid-log phase for 4 h with 2% galactose were analyzed by FACS as described in Materials and Methods. Note that the budding index was probably overestimated in *bed1::URA3* sample because of the cell aggregation observed in these cells. (*B*) Morphology of *bed1::URA3* cells. Phase-contrast micrographs of wild-type (15Daub) and *bed1::URA3* (GY-381) cells grown in YEPD or YEPR. Magnification is the same for both strains. Bar, 10 μm.

before budding. Eight mutations belonging to six complementation groups were isolated from the screening of 25,000 mutagenized colonies (see Materials and Methods for more detailed description of the screening procedure). The first mutation that we characterized was a mutated allele of the previously described *VRP1* gene (Donnelly et al., 1993). This gene encodes verprolin, a proline-rich protein required for proper actin organization. The fact that we recovered *VRP1*, a gene presumably involved in growth polarity and bud emergence, indicated that the screening method was effective for identification of genes involved in growth polarity and bud emergence. We then studied in greater detail the *bed1-1* mutation; the gene defined by this mutation and the encoded protein are the subject of this paper.

A bed1::URA3 Strain Is Defective in Bud Emergence and the Morphogenesis Checkpoint Is Necessary for Its Viability

Although a *GAL1:CLB2-bed1-1* strain was able to grow on dextrose medium (*GAL* promoter repressed) and not on galactose medium (*GAL* promoter induced), a *bed1-1* strain was viable on both media. FACS analysis of nuclear DNA content of a strain overexpressing Clb2 in a *bed1-1* background showed that a large fraction of the cells were arrested with a 4N DNA content (Fig. 1) while Clb2 overexpression in a wild-type background induced only a delay in mitosis (Stueland et al., 1993). Microscopic observation revealed that a large proportion of the cells had more than two nuclei (see below for detailed analysis of the *bed1* phenotype). The *BED1* gene was cloned, sequenced, and a null mutation in the *BED1* gene was created by the one-step disruption method. The cloned gene was shown to be genetically linked to the *BED1* locus (see Materials and Methods and below). We observed that the mutation and the targeted disruption conferred similar phenotypes and therefore used the *bed1::URA3* strain to investigate the *bed1* phenotype in detail. This strain was viable but showed a 30% reduction in growth rate in rich (YEPD) liquid medium compared to the isogenic wild-type strain. The cells were larger than wild-type and almost completely round, having lost the ellipsoidal morphology characteristic of *S. cerevisiae* (Fig. 2 *B*). Using a Coulter Channelizer, *bed1::URA3* cells were shown to be 50% larger than wild-type cells in rich medium (the mean cell volume for *bed1::URA3* cells was 64 fl vs 42 fl for wild-type cells). *bed1::URA3* cells also had defects in cell separation, in that cultures contained clumps of aggregated cells which could not be completely disrupted by sonication (see Fig. 2 *B*). However, treatment with the cell wall–digesting enzyme Zymolyase gave single cells (not shown), indicating that the defect was in cell separation rather than cytokinesis. FACS analysis of *bed1::URA3* cells showed an increase in the proportion of S/G2/M cells in an asynchronous culture in rich liquid medium. A small fraction of the cells scored as greater than 2N in DNA content, presumably because of the cell separation defect (Fig. 2 *A*). In wild-type cells, bud emergence is concomitant with the beginning of S phase as is illustrated by the correlation between the budding index and the percentage of cells that have entered or completed S phase. This was not the case in *bed1::URA3* mutants: in YEPR medium, the percentage of budded cells was lower than the percentage of cells that had entered or completed S phase despite the fact that the budding index was most likely overestimated due to the excessive aggregation associated with the strain (Fig. 2 *A*). These observations were suggestive of a defect in bud emergence conferred by the *bed1::URA3* mutation.

To further characterize this phenotype, small G1 wild-type and *bed1::URA3* cells were isolated by centrifugal elutriation, inoculated into fresh YEPD medium and execution of START, initiation of S phase, bud emergence, and nuclear division were followed (Fig. 3). As previously described (Lew et al., 1992), in the 15D wild-type background, completion of START was followed by S phase and bud emergence within 15–20 min. Nuclear division then occurred 45–50 min later. In *bed1* disruptant cells,

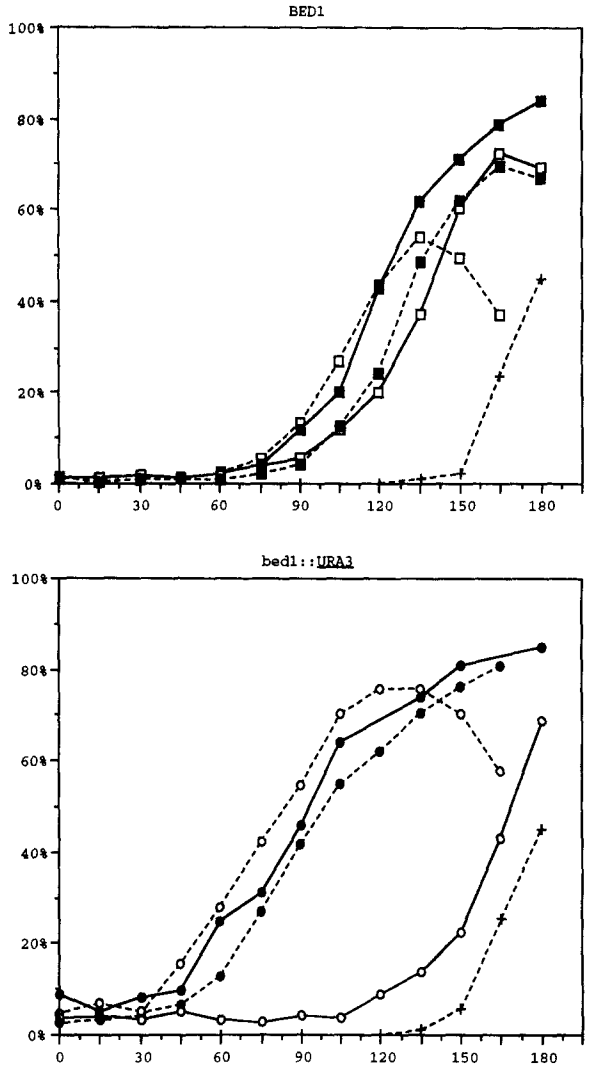

Figure 3. bed1::URA3 cells are defective in bud emergence. Small wild-type (□) or *bed1::URA3* (○) G1 cells were isolated by centrifugal elutriation and the following parameters were evaluated: completion of START (--□-- ; --○--) and S phase (--■-- ; --●--) were determined by FACS analysis; actin polarization (-■- ; -●-), bud emergence (-□- ; -○-), and nuclear division (--+--) were scored by fluorescence microscopy, as described in Materials and Methods.

completion of START occurred sooner than in wild-type cells, presumably because the elutriated population exhibited a larger size than the wild-type controls (not shown). S phase began normally 15–20 min after START but bud emergence was delayed by more than an hour. Nuclear division took place very rapidly after bud emergence, within 10–15 min, suggesting that the morphogenesis checkpoint delays mitosis only until a bud forms to receive the daughter nucleus. Only a small fraction of *bed1::URA3* cells contained more than one nucleus whereas most of the cells overexpressing Clb2 in this background became multinucleated (Fig. 4). This is consistent with the fact that the overexpression of Clb2 or Clb1 is lethal in *bed1-1* or *bed1::URA3* cells (Fig. 1 *A* and Fig. 2 *B*; not shown). In a synchronized culture, these cells went through S phase and mitosis before bud emergence and died with more than two nuclei (not shown). The disruption of the *BED1* gene in the context of the $cdc28^{F19A18}$ mutation (where *CDC28* is mutated so as to be no longer subject to negative regulatory phosphorylation) was not lethal but a large fraction of the cells were multinucleated (Fig. 4). It was difficult to quantify the percentage of multinucleated cells in these different strains because of the cell aggregation phenotype, but it was clear that more multinucleated cells were detected when Clb2 was overexpressed or Cdc28 was not phosphorylatable. It was also apparent that, in *bed1::URA3* cells, nuclear division occurred very rapidly after bud emergence, in that daughter nuclei were observed even in very small buds while nuclear division took place in wild-type cells when buds were much larger (Fig. 4). We

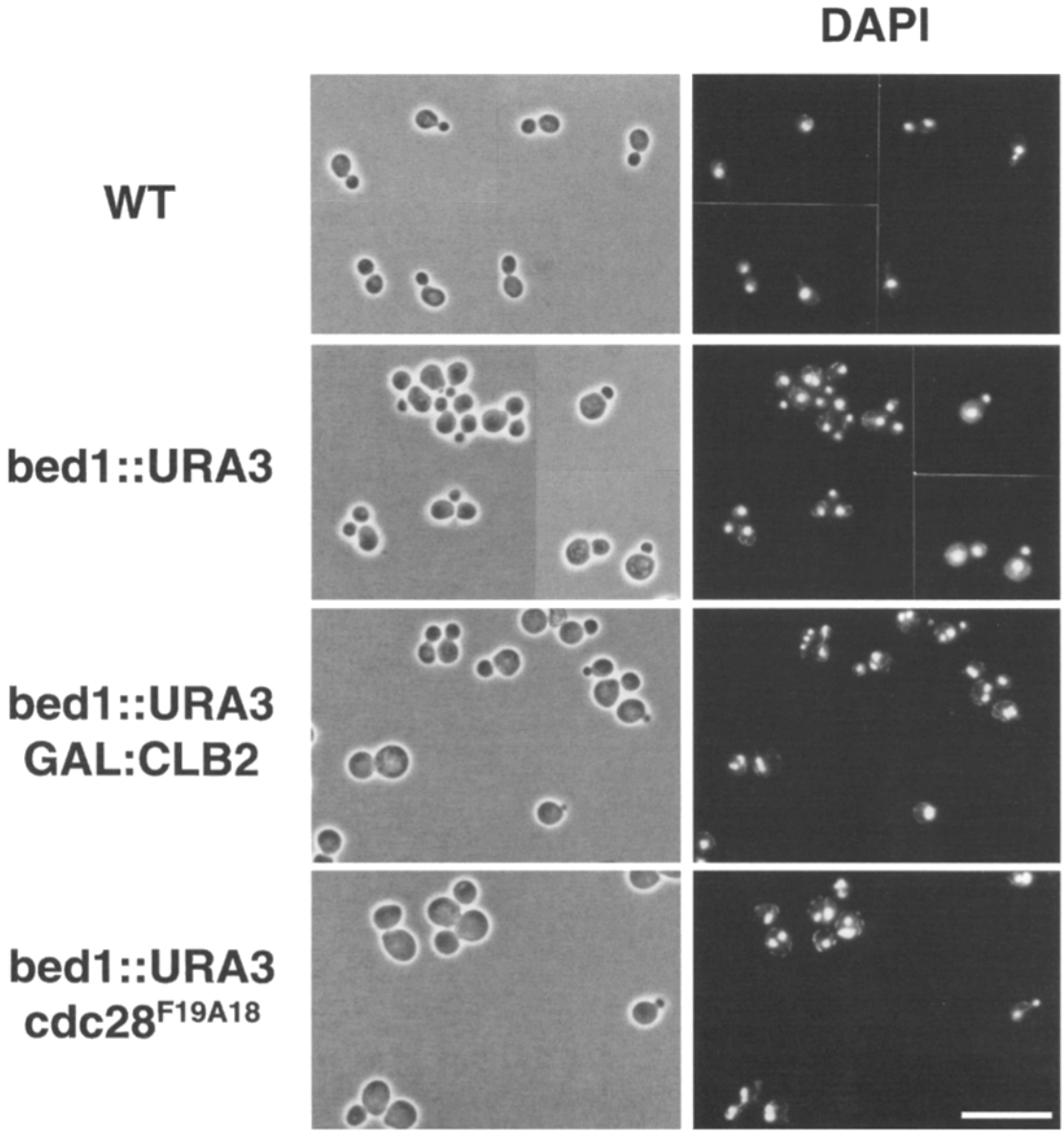

Figure 4. The viability of *bed1::URA3* cells depends on the integrity of the morphogenesis checkpoint control machinery. Nuclei were visualized by staining cells with DAPI: (*A*) wild-type (15Daub in YEPD); (*B*) *bed1::URA3* (GY-381 in YEPD); (*C*) *bed1::URA3-GAL1:CLB2* (GY-382 after a 4 h induction with 2% galactose in YEPR); (*D*) *bed1::URA3-cdc28::LEU2-*$CDC28^{F19A18}$*(TRP1)* (GY-449 in YEPD). Note that the fields are not representative of the percentage of multinucleated cells in the different strains. Magnification is the same for all the strains. Bar, 10 μm.

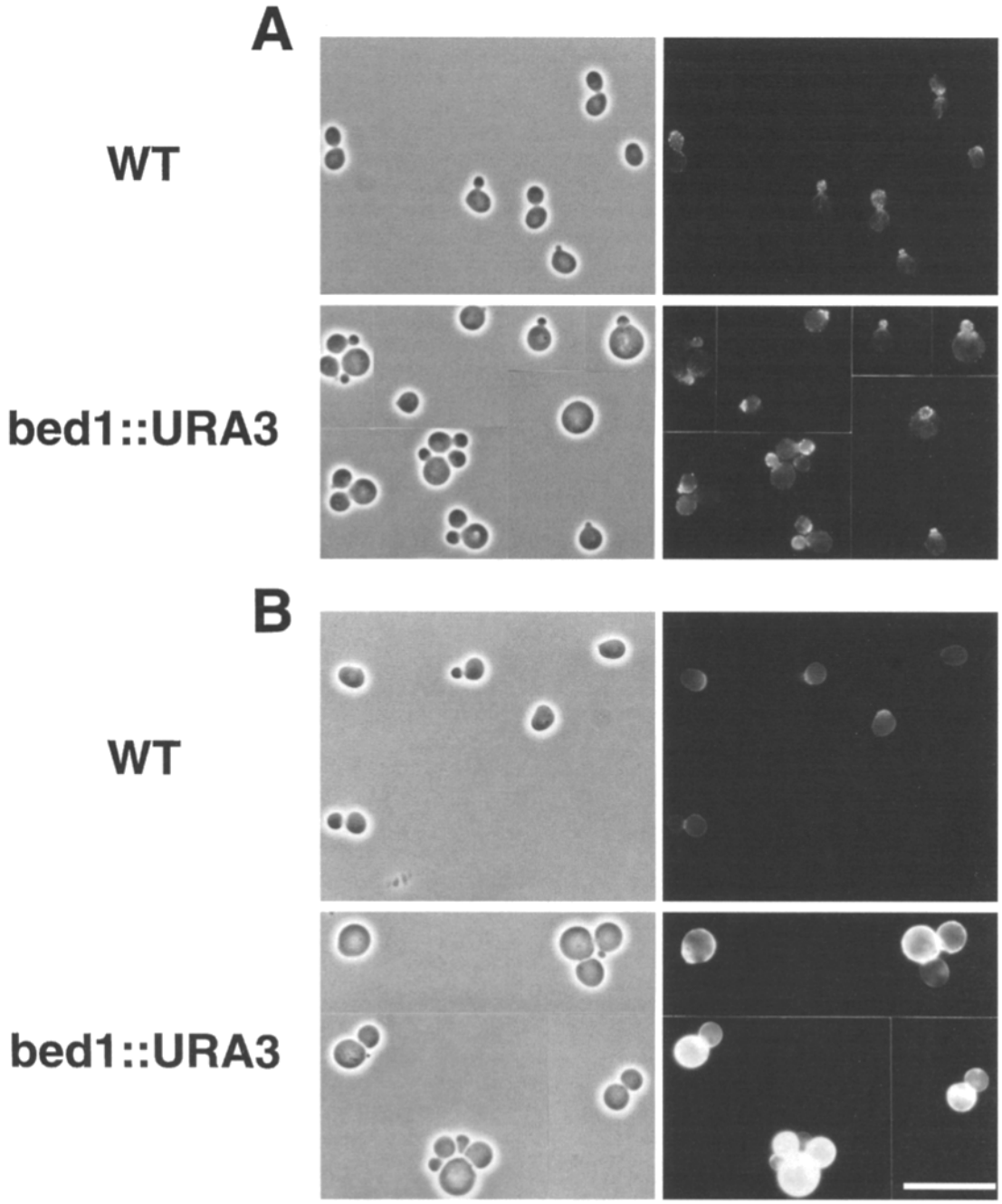

Figure 5. Actin and chitin localization in *bed1::URA3* cells. Wild-type (15Daub) and *bed1::URA3* (GY-381) cells grown in YEPD were fixed with formaldehyde and stained with rhodamine-phalloidin to visualize actin (*A*) or with calcofluor to detect chitin (*B*). Magnification and exposure time are the same for both strains. Bar, 10 μm.

concluded from these experiments that the *BED1* gene was required for timely bud emergence, that the morphogenesis checkpoint is functional and that the viability of *bed1::URA3* cells depends on the integrity of this checkpoint control machinery.

bed1::URA3 Cells Have Defects in Polarized Growth Although Actin Is Properly Polarized

The fact that *bed1* mutant cells are delayed in bud emergence, are large, and have an unusually round morphology, suggested that they might be defective in polarized growth during the cell cycle. This type of phenotype is often associated with an inability to properly organize the actin cytoskeleton (see Discussion). We investigated this possibility by looking at actin localization by rhodamine-phalloidin staining of *bed1* mutant cells. As shown in Fig. 5 *A*, actin staining revealed a pattern similar to that observed in wild-type cells: actin rings were observed at the pre-bud site and after bud emergence, actin patches were found exclusively in the buds and actin cables were oriented toward the tips of the buds. Finally actin patches

were relocalized to the necks of the buds during cytokinesis. We also observed, as with wild-type cells, that actin patches were concentrated to the tip of the growth projection (shmoo) when *bed1* mutants were treated with the mating pheromone α factor (not shown).

We then determined the timing of polarization of the actin cytoskeleton during the cell cycle in a synchronized culture (Fig. 3). *bed1* mutant cells began to undergo actin polarization within 5 min after completing START, as in wild-type cells. We concluded, therefore, that actin was properly polarized at the appropriate time during the cell cycle, indicating that the *bed1* phenotype does not result from an inability to reorganize the actin cytoskeleton at the G1/S phase boundary.

On the other hand, staining of *bed1* mutants with calcofluor, a stain for chitin, which is normally found concentrated in the neck region of a budded cell and in "scars" on cells where previous buds were located, revealed that chitin was now completely delocalized and deposited at elevated levels (Fig. 5 *B*). One interpretation of this phenotype is that *bed1* mutants are defective in polarized secretion required for proper localization of chitin synthase despite the fact that there is no obvious defect in polarization of the actin cytoskeleton.

Growth polarity can be directly visualized by pulse-labeling cells with FITC-ConA, which binds mannose residues from the cell wall and chasing in the absence of FITC-ConA (for a more detailed description of this method, see Lew and Reed, 1993). Exponentially growing wild-type and *bed1::URA3* cells were pulse labeled and fixed after a chase of one generation equivalent in fresh medium. Daughter cells originating from labeled buds (cells with an unlabeled birth scar) were scored for staining patterns characteristic of isotropic growth (uniform staining; see, for example, cell *1* in Fig. 6 *A*) or apical growth (staining that fades out toward one end of the cell; see, for example, cell *2* in Fig. 6 *A*). As previously described (Lew and Reed, 1993), ~40% of the daughter cells from a wild-type population in YEPD medium exhibited polarized growth (169 out of 449 daughter cells). Among the cells exhibiting a pattern indicative of polarized growth, 15% showed a partial gradient of the staining where the pole of the cell was still detected (see cell *3* in Fig. 6 *A*; 27 out of 169). On the other hand, most of the *bed1::URA3* daughter cells (~60%; 275 out of 452 daughter cells) exhibit a uniform staining indicative of completely isotropic growth (cell *4*) and no daughter cells with completely unlabeled poles indicative of apical growth were observed. However, ~15% of these cells (66 out of

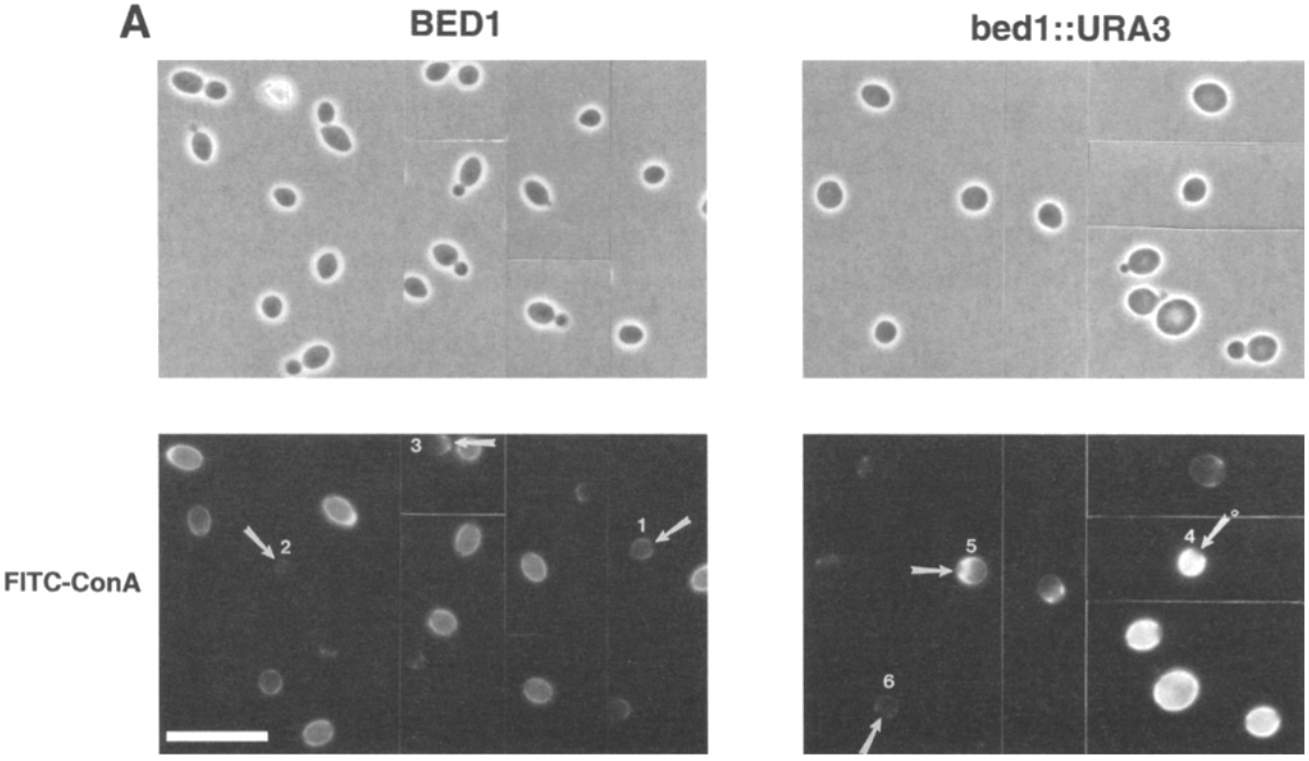

Figure 6. FITC-ConA pulse labeling of wild-type and *bed1* cells. (*A*) Wild-type (DLY-005) and *bed1* mutant (GY-647) diploid cells were pulse labeled with FITC-ConA for 15 min and after a chase with fresh medium during one generation time, cells were fixed and observed by fluorescence microscopy. Daughter cells generated from labeled buds with an unlabeled birth scar (indicated by an arrow) were scored for uniform staining indicative of an isotropic growth (cell *1*), for staining that fades completely out toward the pole opposite from the unlabeled birth scar, indicative of polarized growth (cell *2*) or for an incomplete or partial gradient toward the end of the daughter cell (cell *3*). In the mutant population, daughter cells exhibiting uniform staining (cell *4*) or an incomplete gradient toward one pole of the cell (cell *5*) could be observed along with cells showing a weak uniform staining with brighter signal around the birth scar (cell *6*). Bar, 10 μm. (*B*) Confocal microscopy was used to characterize the staining of the same cells in greater detail. Examples of staining indicative of polarized growth in wild-type cells are shown on the left. Mutant daughter cells exhibiting weak uniform staining with brighter staining around the birth scar or partial fade-out staining are shown on the right. Bar, 5 μm.

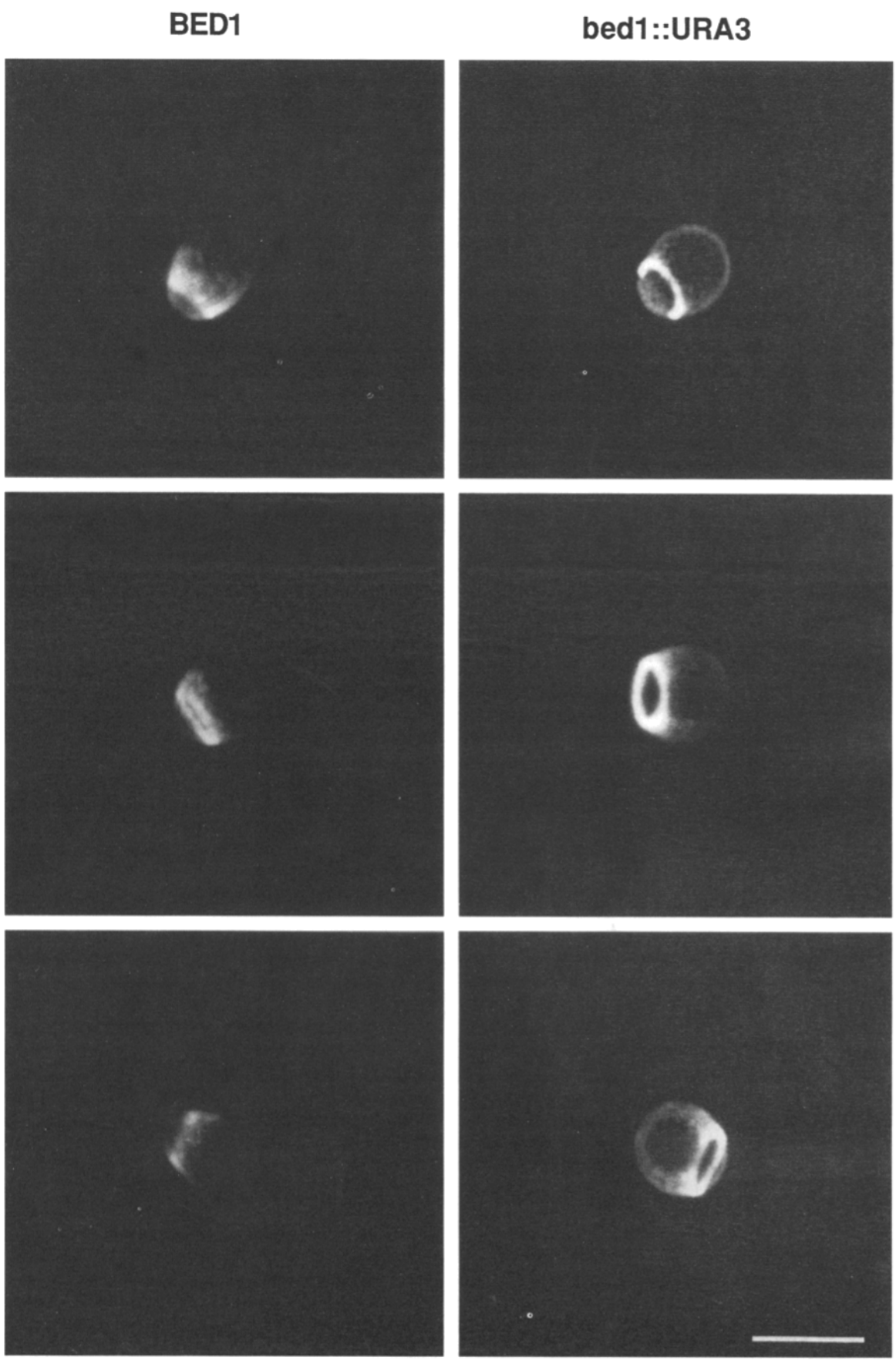
B
BED1
bed1::URA3

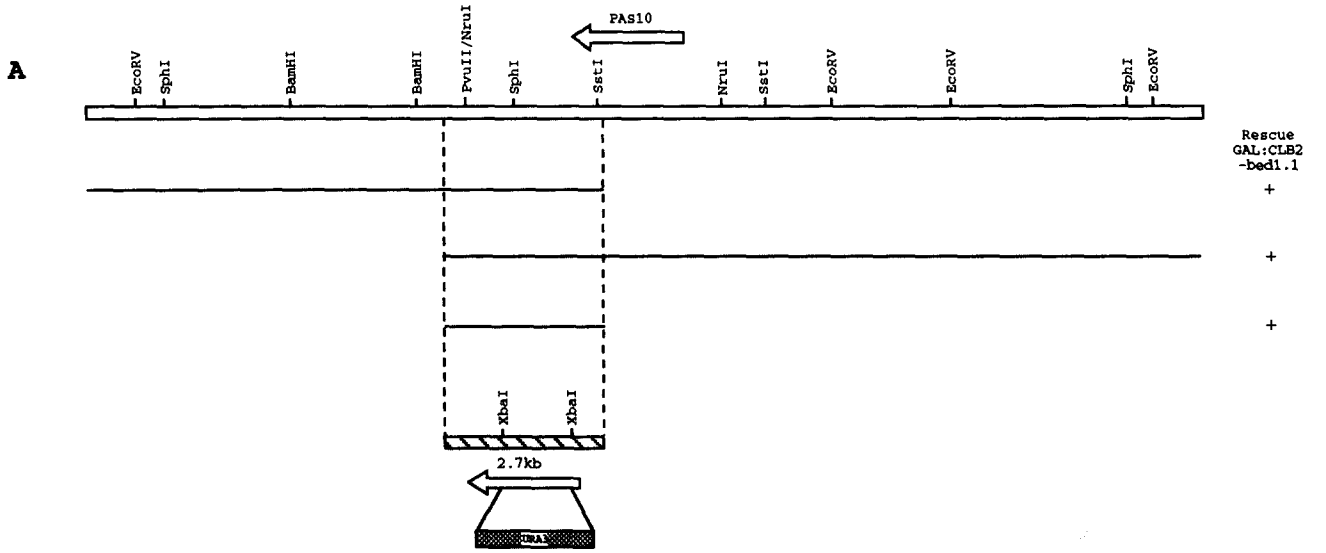

B

```
-645                                          -615
GGT ATC ATC CAT GAA TAT AGG CTG ATC AAA GAA GCA GCA GGC TAC TTA TTA AGT GTT CTA
-585                                          -555
AGT ATG CAT GAA GTG AAC ACT AAT AAT AAA AAA GGA GAC GTT GGA TCT CTC TTG AAT ACG
-525                                          -495
TAC AAT GAT ACT GTT ATA GAG ACT TTG AAG AGA GTT TTT ATA GCG ATG AAT AGA GAT GAT
-465                                          -435
TTA CTT CAA GAA GTG AAG CCA GGC ATG GAC CTG AAA AGA TTT AAA GGA GAA TTT TCG TTT
-405                                          -375
TGA TAT GGT TCT CCG CAA TTT TAT GTT CTC GCA TCA CTG CCC AAA TTC ATT AGC ATT AGC
OPA
-345                                          -315
AGT ACA AGC TAT CCT ATA TAT AAG GCA ATA AAA AAT CTT ATA AAT ACT ATC AGC AAG ATT
-285                                          -255
TCA ACC CTT GGA AAA ACA TGC ATT CAA AGG TCA TAA TTG CTG CTC TAT TTT ACA AGT CGT
-225                                          -195
CCA TAA TGA CAT TTC TCT TTG ATT ATT TTC TTG TTT TTT CGC TCT TCT CAA GTG GAT GTT
    OCH OPA
-165                                          -135
ACA TAA CAA ACA AAA CAG AAA AAA TTG TTT AAA TAT AAA GTT TAA AAG TTA TCT TTG ATT
  OCH                                           OCH
-105                                          -75
CCG CAC CTG AAT TTT TGG ATT GAA GGC CAA AGG AGG TTT ATC AGG GAG AGA AAA GCT CTC
-45                                           -15
TAT TTA TTT TTA TAA GGA ATA ATT GTG CAT GTA CAA CTA TAC AAT ATG TCT AGT GTA CCT
            OCH                                                MET ser ser val pro
+16/6                                         +46/6
TAT AAT TCC CAA CTT CCT ATA TCC AAC CAT CTA GAG TAC GAT GAA GAT GAA AAG AAG AGC
                                              XbaI
tyr asn ser gln leu pro ile ser asn his leu glu tyr asp glu asp glu lys lys ser
+76/26                                        +106/36
AGA GGC TCA AAA CTA GGC CTG AAA TAT AAA ATG ATA TAC TGG AGG AAA ACT TTA TGC AGT
arg gly ser lys leu gly leu lys tyr lys met ile tyr trp arg lys thr leu cys ser
+136/46                                       +166/56
TCG CTA GCG AGA TGG AGA AAG CTA ATA CTA TTA ATA TCT TTA GCT TTG TTT TTA TTC ATA
ser leu ala arg trp arg lys leu ile leu leu ile ser leu ala leu phe leu phe ile
+196/66                                       +226/76
TGG ATA AGC GAT TCC ACC ATA AGC AGA AAT CCA TCT ACC ACA AGT TTT CAA GGC CAA AAT
trp ile ser asp ser thr ile ser arg asn pro ser thr thr ser phe gln gly gln asn
+256/86                                       +286/96
AGT AAC GAT AAT AAG TTG AGT AAT ACT GGT TCT AGC ATC AAC TCC AAA AGA TAT GTA CCA
ser asn asp asn lys leu ser asn thr gly ser ser ile asn ser lys arg tyr val pro
+316/106                                      +346/116
CCA TAT TCT AAG AGA TCA AGA TGG TCG TTT TGG AAT CAA GAT CCT AGG ATT GTC ATT ATA
pro tyr ser lys arg ser arg trp ser phe trp asn gln asp pro arg ile val ile ile
+376/126                                      +406/136
TTA GCG GCA AAC GAA GGT GGT GGT GTA TTG AGG TGG AAA AAT GAG CAA GAA TGG GCT ATC
leu ala ala asn glu gly gly gly val leu arg trp lys asn glu gln glu trp ala ile
+436/146                                      +466/156
GAA GGC ATA TCA ATA GAA AAT AAG AAG GCC TAT GCG AAG AGA CAT GGA TAT GCG TTG ACT
glu gly ile ser ile glu asn lys lys ala tyr ala lys arg his gly tyr ala leu thr
+496/166                                      +526/176
ATC AAG GAT TTG ACA ACG TCC AAA AGA TAC TCT CAC GAA TAC AGA GAG GGT TGG CAA AAA
ile lys asp leu thr thr ser lys arg tyr ser his glu tyr arg glu gly trp gln lys
+556/186                                      +586/196
GTA GAT ATA TTG AGA CAG ACG TTC AGG GAG TTT CCT AAT GCA GAA TGG TTC TGG TGG TTG
val asp ile leu arg gln thr phe arg glu phe pro asn ala glu trp phe trp trp leu

+616/206                                      +646/216
GAC CTG GAT ACT ATG ATA ATG GAG CCT TCT AAA TCA TTA GAA GAA CAT ATT TTC GAC AGA
asp leu asp thr met ile met glu pro ser lys ser leu glu glu his ile phe asp arg
+676/226                                      +706/236
TTG GAA ACT CTG GCT GAC AGA GAA TTG AAA AGT TTT ATT CCC CTA AAC CTA AGA GAC GAC
leu glu thr leu ala asp arg glu leu lys ser phe ile pro leu asn leu arg asp asp
+736/246                                      +766/256
ATA CCC TAT GTC GAT TAT TCA GAG GAA ATG GAG TTT CTA ATA ACA CAA GAT TGT GGA GGC
ile pro tyr val asp tyr ser glu glu met glu phe leu ile thr gln asp cys gly gly
+796/266                                      +826/276
TTC AAT TTG GGC TCA TTT CTG ATA AAA AAT AGC GAA TGG TCT AAG CTG CTT CTA GAT ATG
                                                                 XbaI
phe asn leu gly ser phe leu ile lys asn ser glu trp ser lys leu leu leu asp met
+856/286                                      +886/296
TGG TGG GAC CCC GTT CTG TAT GAA CAA AAA CAT ATG GTT TGG GAA CAT AGA GAA CAA GAT
trp trp asp pro val leu tyr glu gln lys his met val trp glu his arg glu gln asp
+916/306                                      +946/316
GCG TTA GAG GCA TTA TAT GAA AAC GAA CCG TGG ATT CGT TCG AGA ATA GGA TTT TTG CCC
ala leu glu ala leu tyr glu asn glu pro trp ile arg ser arg ile gly phe leu pro
+976/326                                      +1006/336
TTA AGA ACG ATC AAT GCA TTC CCA CCG GGA GCA TGC TCT GAA TAC AGT GGT GAC TCA AGA
leu arg thr ile asn ala phe pro pro gly ala cys ser glu tyr ser gly asp ser arg
+1036/346                                     +1066/356
TAC TTT TAC AGT GAG AAA GAC CAT GAT TTT GTT GTG AAT ATG GCC GGA TGC AAT TTT GGC
tyr phe tyr ser glu lys asp his asp phe val val asn met ala gly cys asn phe gly
+1096/366                                     +1126/376
AGA GAT TGC TGG GGC GAG ATG CAG TAC TAC ACC ACT TTA ATG GAA AAA CTG AAT AGG AAA
arg asp cys trp gly glu met gln tyr tyr thr thr leu met glu lys leu asn arg lys
+1156/386                                     +1180/393
TGG TAC ACG AGA TTT TTC TTC CCA TAA AAT GGA AGT TAT CAA TAT TGT AAA GAG AAG CAT
trp tyr thr arg phe phe phe pro OCH
+1216                                         +1246
TTA CAA GCT TTT ATT TTT CTT TTT AAT TTC CAC TAC TGG TTC TGC TTT AAA ATG TTG TTT
+1276                                         +1306
TAT AAT TTA TGT ACA TTT AGG CCT ATA GAA GAT TCT TTC AAT AAT ATG CTA CAC ATT CTT
+1336                                         +1366
TTA TTT TTC CAT CAT ATG TTG GAG TTT ATG CCT CCT CGG CAG GAG TTG GGC GGT GCG AAG
+1396                                         +1426
AGA AGA AAA AGA GTG AAA CTA AAA AAA GGA ATC TGC CTT TGC ATA AGT TCA AAA GTG CAA
+1456                                         +1486
TTT TAG TGT TGG ATT TAA ACG GGA AAA ATT GAA ATG GCC ATC GAA ACA ATA CTT GTA ATA
+1516                                         +1546
AAC AAA TCA GGC GGA CTA ATC TAT CAG CGG AAT TTT ACC AAC GAC GAA CAG AAA TTG AAC
+1576                                         +1606
AGC AAT GAA TAC TTA ATT CTT GCT AGT ACA CTG CAC GGT GTA TTC GCC ATC GCG AGC CAG
+1636                                         +1666
CTG ACT CCG AAG GCA TTA CAG CTA ACT CAA CAA ACG AAC ATC GAA AAT ACC ATC CCA TAT
+1696                                         +1726
ATA CCT TAC GTG GGC ATG TCC AGC AAT AGG AGC GAT ACA AGA AAT GGA GGT GGC AAT AAC
+1756                                         +1786
AAC AAA CAC ACT AAT AAT GAA AAA CTG GGC AGT TTT AAA GGA GAT GAT TTT TTC AAA GAA
+1816                                         +1846
CCA TTT ACG AAC TGG AAC AAG AGC GGA TTG AGA CAA CTA TGC ACG GAT CAG TTC ACG ATG
+1876                                         +1906
TTC ATA TAT CAG ACC CTA ACC GGC CTG AAG TTT GTC GCT ATC AGC TCC AGC GTC ATG CCC
+1936
CAG AGA CAG CCA ACT
```

Figure 7. Identification and molecular cloning of the *BED1* gene. (*A*) Physical map of the DNA fragment able to rescue the lethality on galactose of the GY-159 strain. The disruption of the *BED1* gene with the *URA3* marker is also schematized. (*B*) Sequence of the *BED1* gene. The sequence around the ATG is underlined and is in good accordance with the consensus sequence 5′-(A/Y)A(A/Y)A(A/Y)AATGTCT-3′ (Hinnebusch and Liebman, 1991). Sequences for termination of transcription (5′-TAG...TATGTTG...TTT-3′) were also found after the STOP codon. The sequences upstream from the *BED1* gene were identical to the 3′ end of the sequence of the *PAS10* gene (YSCPAS10P in Genebank; Van Der Leij et al., 1993). The amino-terminal hydrophobic region of the Bed1 protein is indicated in italics. These sequence data are available from GeneBank/EMBL/DDBJ under accession number U31446.

452) exhibited a partial fade-out staining with a decreasing gradient of the staining to one end of the cell but with the pole still labeled (see for example, cell *5* in Fig. 6 *A*) and ~25% (111 out of 452) showed a faint uniform staining with a zone of strong staining around the birth scar (see, for example, cell *6* in Fig. 6 *A*). We used confocal microscopy to analyze the fade-out staining in greater detail (Fig. 6 *B*). While no staining could be detected at the opposite pole of the unlabeled birth scar in wild-type cells, the end of *bed1::URA3* daughter cells was always stained, suggesting that

the apical growth, when it occurs, is defective or incomplete. Examination of cells with a stronger signal around the birth scar (cell *6* in Fig. 6 *A*) showed that the pattern is consistent with staining of a region very close to the scar itself but without any gradient toward the pole of the cell. Our interpretation is that growth cannot occur in this region for mechanical reasons and therefore the signal cannot be diluted during bud growth and appears as a narrow ring of heavily stained cell wall. The fact that we could still detect in some cells a partial gradient toward one pole of the cell (~15% of daughter cells) suggests that growth may be partially polarized at some point of the budding phase. Taken together, these results suggest that *bed1::URA3* cells exhibit some growth polarity but that apical growth is not as efficient as in wild-type cells.

Molecular Characterization of the BED1 Gene: BED1 Shows Similarity to an S. pombe Gene Encoding an α-1,2-Galactosyltransferase

The gene encoding Bed1 was cloned by complementation of the *GAL1:CLB2-bed1-1* mutant strain (GY-159) using a centromeric yeast genomic DNA library and two plasmids containing a 2.7-kb overlapping region were recovered (Fig. 7 *A*). We detected one large open reading frame (ORF) in this region with a capacity for encoding a protein of 393 amino acids (Fig. 7 *B*). Examination of the sequence of the *BED1* gene showed a stretch of hydrophobic amino acids in the NH_2-terminal portion of the ORF (residues 47 to 67; Fig. 7 *B*). The inferred structure of Bed1 was reminiscent of the organization of type II membrane proteins: a short NH_2-terminal cytosolic domain, a unique hydrophobic transmembrane domain (15–20 aminoacids) and a large luminal COOH-terminal domain (for review see High and Dobberstein, 1992).

BED1 had similarity to the recently cloned *gma12*$^+$gene of *S. pombe* (Chappell et al., 1994). The two proteins are similar in their predicted luminal domains: 4 regions that show ~30% identity and up to 70% similarity (Fig. 8). The structures of these two proteins are different in that, although they both have type II membrane protein structure, the cytoplasmic domain of Bed1 is larger (45 amino acids) than the corresponding domain of gma12p (only two amino acids amino terminal to the transmembrane domain). The *gma12*$^+$ gene encodes an α-1,2-galactosyltransferase involved in the synthesis of the *S. pombe* cell wall which, in contrast to that of *S. cerevisiae*, contains glycoproteins with galactose residues. More recently, two putative ORF homologous to gma12p were detected on chromosome I of *S. pombe*. Therefore, *gma12*$^+$ belongs to a highly conserved family of proteins that are conserved along their entire lengths in the fission yeasts *S. pombe* and *S. octosporus* (Fig. 8; Chappell, T., personal communication).

We also noticed that Bed1 is even more homologous to a previously unidentified *S. pombe* partial ORF present adjacent to the vacuolar H^+-ATPase, subunit B gene (Fig. 8). Analysis of the sequences available shows that the homology between *Bed1* and this partial ORF is significantly greater than that between Bed1 and gma12p (see Fig. 8). The structure of this ORF is also more similar to the structure of Bed1 in that the putative cytoplasmic domain contains ~40 amino acids. However, the role of the protein represented in part by this ORF is not known. The possible implications of these homologies will be discussed below.

Bed1 Is a Type II Membrane Protein Localized in the Endoplasmic Reticulum

Since the analysis of *bed1::URA3* cells suggested a role in polarized secretion and Bed1 had a predicted structure organization consistent with a membrane protein, we determined the intracellular localization of Bed1. We introduced a COOH-terminal triple influenza hemagglutinin ([HA]3X)-tagged version of Bed1 into *bed1::URA3* cells. The HA-specific 12CA5 monoclonal antibody detected a

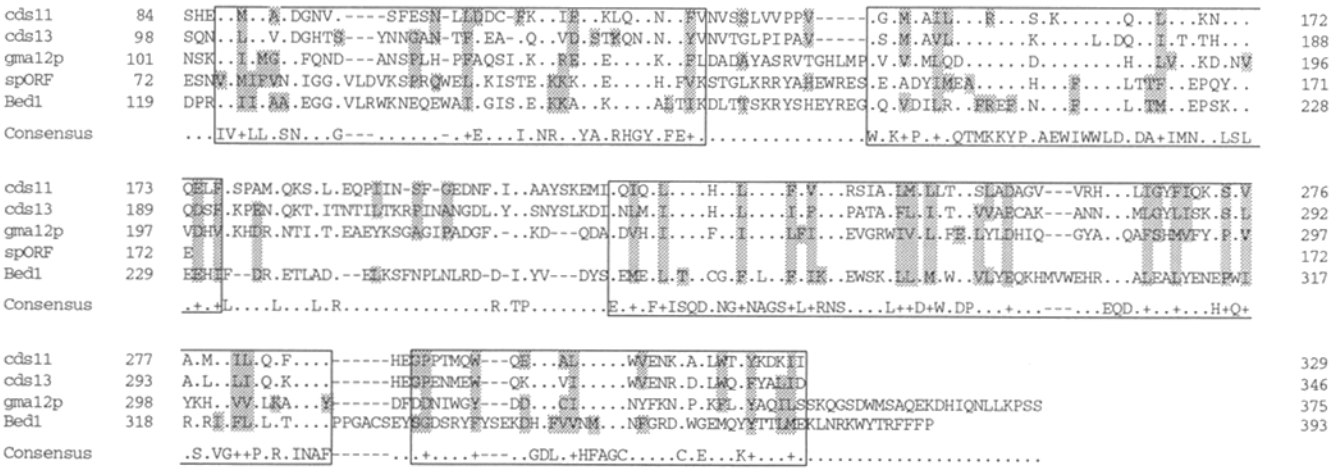

Figure 8. Homologies between *BED1* and *gma12*$^+$, an *S. pombe* gene encoding an α-1,2-galactosyltransferase. The search for sequences homologous to Bed1 was performed at the National Center for Biotechnology Information (NCBI) through the GENINFO (R) BLAST Network Service (Blaster) (Altschul et al., 1990). Four *S. pombe* ORFs were identified: gma12p (SPA12GATR; accession number zQ09174), two ORFs on chromosome I (cds11 and cds13; accession number z49811) and a previously unidentified partial ORF (spORF) located 5′ from the vacuolar H^+-ATPase, subunit B gene (SPVATPB). The alignment of the 5 ORFs was established with the following rules: G=A=P=S; S=A=T; R=H=K; D=E; Q=N; M=I=L=V=F; F=W=Y.

doublet on Western blots of approximate molecular mass of 50 kD, in good agreement with the predicted molecular weight of the fusion protein (46 kD for Bed1 and 4 kD for the [HA]3X tag) (Fig. 9 *A*). The HA-tagged version of *BED1* was able to rescue the defects associated with the disruption of *BED1* (not shown). Thus, we concluded that the fusion protein was functional. Crude fractionation of extracts containing intact membrane structures showed that Bed1[HA]3X was present in the low speed fraction (P13) enriched for endoplasmic reticulum, nuclear envelope, vacuoles, and plasma membrane. Kar2, a luminal protein of the ER (Rose et al., 1989), was also mainly present in this fraction, as expected. We also showed that, unlike Kar2, Bed1 was tightly associated with membranes: Bed1 remained membrane associated after treatment of the membrane fraction with carbonate pH11.0 but not after treatment with detergents (not shown). Moreover, only the NH_2-terminal portion of Bed1 was sensitive to proteolysis by proteinase K when the protein was associated with intact membranes, suggesting that the first 45 amino acids are likely to be cytosolic in intact cells (not shown). Based on these criteria, we concluded that Bed1 is a type II integral membrane protein.

We were unable to detect Bed1[HA]3X by immunofluorescence when the fusion protein was expressed under the control of its native promoter (not shown). Therefore, we constructed a strain containing the tagged protein under control of the constitutive GAP promoter (GY-718), yielding a 20-fold increase in the amount of Bed1 protein, as observed by Western blot (Fig. 9 *A*). Since it has been shown that, in some cases, overexpression of proteins of the secretory pathway can lead to a mislocalization due to saturation effects, we verified that Bed1 had the same fractionation profile when overexpressed as when it was expressed under control of its own promoter (Fig. 9 *A*). We observed an immunofluorescence staining pattern consistent with an ER localization of the protein: the signal was perinuclear with some extensions into the cytoplasm. This pattern was similar to the immunolocalization of Kar2, a luminal protein of the endoplasmic reticulum (Rose et al., 1989). We also observed that Bed1 colocalized with Kar2 in individual cells (not shown). These data taken together suggest that Bed1 is a type II integral membrane protein of the endoplasmic reticulum and support the hypothesis, based on homologies with *gma12*$^+$, that Bed1 is a galactosyltransferase and that the switch to polarized secretion might require galactosyl modification of particular proteins or lipids during transit through the endoplasmic reticulum.

Discussion

The *BED1* gene was identified based on its involvement in bud emergence and polarized growth in *S. cerevisiae*. Although impaired, cells disrupted for *BED1* are viable, suggesting either that this gene encodes an important but nonessential function, or that *BED1* is redundant with another related gene. Bud emergence was strongly delayed, occurring only 1 h after initiation of S phase in *bed1::URA3* cells while these two events were tightly coupled in wild-type cells. On the other hand, nuclear division took place immediately after bud emergence, indicating a tight coupling between these two events in *bed1* mutant cells. However, *bed1* cells became multinucleated when the mitotic form of Cdc28 was hyperactivated by either the overexpression of the mitotic cyclins Clb1 or Clb2 or by mutation of Tyr19, the regulatory phosphorylation site of Cdc28. Lew and Reed (1995*a*) have shown that, while the G2 delay induced by defects in growth polarity or budding can be completely abolished by Clb1 or Clb2 overexpression, the *cdc28*^{F19} mutation only reduces the delay but cannot eliminate it completely. This accounts for the observation that a *bed1::URA3-cdc28*^{F19A18} strain is viable while overexpression of Clb2 in a *bed1::URA3* background is lethal. Taken together, these observations suggest that the viability of *bed1* cells depends on the morphogenesis checkpoint machinery which is able to delay mitosis in the absence of budding in order to maintain the coordination between the nuclear division cycle and the budding cycle. In fact, the dependence of the *bed1* mutant on the morphogenesis checkpoint for survival is the most convincing demonstration of the importance of this regulatory system in the yeast life cycle. Finally, cells disrupted for *BED1* exhibited morphological aberrations, losing the ellipsoidal shape characteristic of *S. cerevisiae* and being larger than wild-type cells. In addition, *bed1* cells had defects in cell separation as indicated by a tendency to form aggregates in liquid medium.

The delayed bud emergence, the morphological and morphogenetic phenotypes observed in *bed1::URA3* cells (increased size, round cell shape, and delay in bud emergence) could be a result of defects in secretion or the generation of growth polarity by analogy with other morphogenesis mutants (for reviews see Bretscher et al., 1994; Welch and Drubin, 1994). Disorganization of the actin cytoskeleton and delocalized deposition of chitin are usually phenotypically coupled, presumably because proper actin function is required for polarized secretion and therefore for budding. In *bed1::URA3* cells, actin polarization after START and actin reorganization at cytokinesis occurred on schedule. Surprisingly, however, chitin deposition was greatly increased and completely delocalized, indicating that *bed1* cells have defects in polarized growth. Moreover, a more direct evaluation of growth polarity by in vivo pulse labeling with FITC-ConA showed that *bed1::URA3* cells are defective in the most polarized form of growth, growth directed to the bud tip or apical growth. Some residual growth polarity was observed, explaining why *bed1::URA3* cells are viable and suggesting that another gene redundant with *BED1* might be responsible for this activity. From these observations, we suggest that *bed1* cells are impaired in directing secretory vesicles to the bud site but not in secretion per se, and that Bed1 is part of a pathway that is downstream or parallel to the actin pathway; both pathways being necessary for proper delivery of secretory vesicles to the bud site during bud emergence and to the bud neck during cytokinesis and cell separation.

A role in polarized secretion is also consistent with the intracellular localization of Bed1. Crude fractionation of whole cell lysates showed that Bed1 was present in a low speed fraction containing endoplasmic reticulum, vacuoles, nuclear envelope, and plasma membranes. Biochemical experiments indicated that Bed1 was an integral type II membrane protein with a small NH_2-terminal cytoplasmic

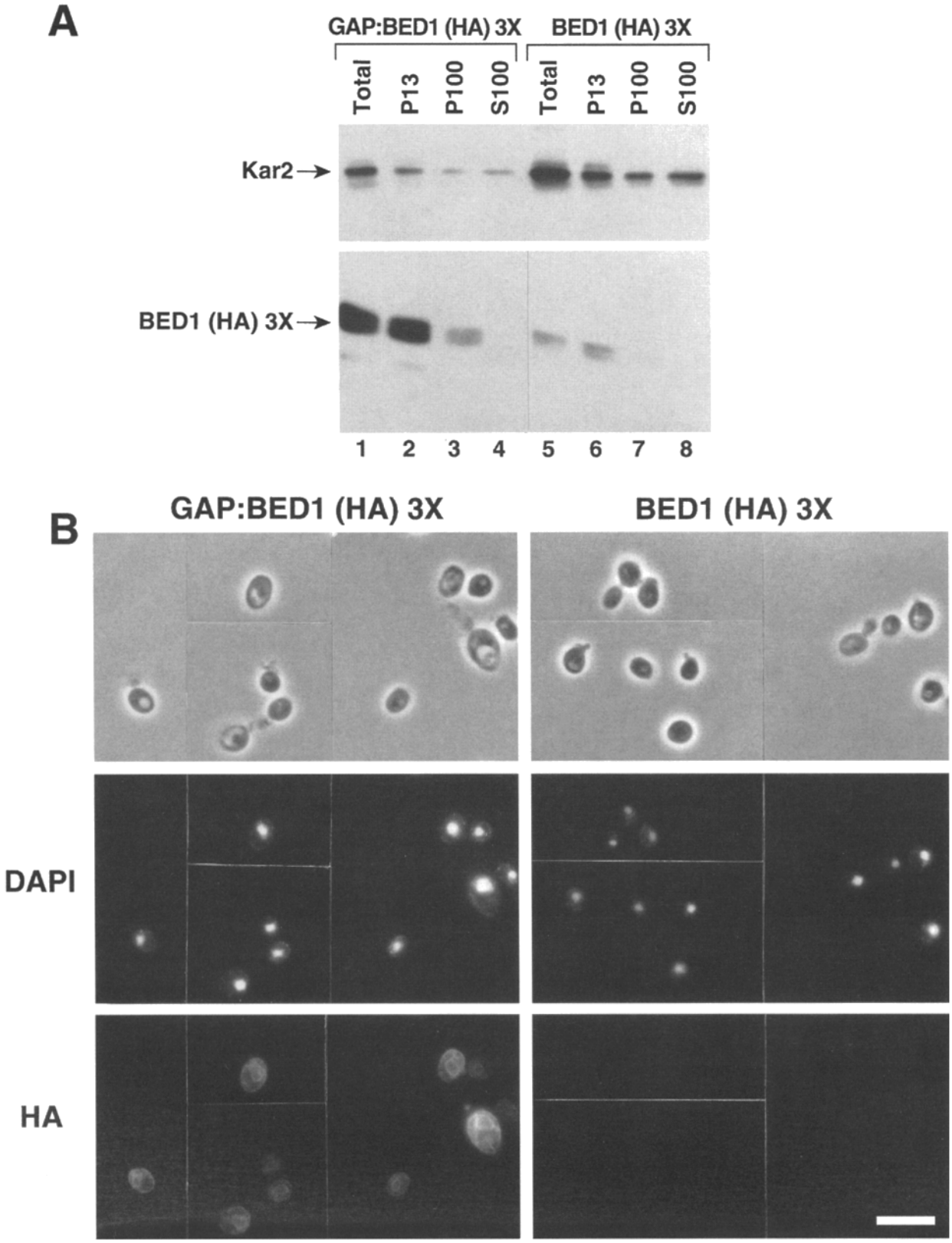

Figure 9. Bed1 is a membrane protein localized in the endoplasmic reticulum. (*A*) Bed1 is present in an ER-enriched fraction. Total protein extracts (*TOTAL*) containing intact membrane structures were subjected to a crude fractionation procedure: the P13 fraction is enriched for membranes from the endoplasmic reticulum, the vacuoles, the plasma membrane and the nuclear envelope; the P100 fraction is enriched for Golgi membranes; the S100 fraction contains soluble proteins. The Bed1[HA]3X protein was detected by Western blot with the 12CA5 mouse monoclonal antibody and Kar2 with a rabbit polyclonal antibody. Note that twice as much volume of GY-723 (*BED1*[HA]3X) was loaded compared to GY-718 (GAP:*BED1*[HA]3X). It was estimated by densitometric scanning of different exposures of the Western blots that 40% of Kar2 was in the P13 fraction, 20% in the P100, and 20% in the S100 fraction. The same kind of measurement gave for Bed1 90%, 10%, and less than 1% in fractions P13, P100, and S100, respectively. (*B*) Immunolocalization of Bed1. GY-718 (containing GAP:*BED1*[HA]3X) and GY-716 (containing GAP:*BED1* as a negative control) cells grown in YEPD were stained with DAPI to visualize the nuclei and at the same time with the 12CA5 antibodies to detect the Bed1 fusion protein. Magnification and exposure time are the same for both strains. Bar, 5 μm.

domain and COOH-terminal luminal domain. The predicted structure of the protein was in agreement with this conclusion since Bed1 contained a putative hydrophobic transmembrane domain in the NH_2-terminal portion of the protein (amino acids 47–67). We were not able to detect an epitope-tagged version of the protein expressed from its own promoter by immunofluorescence because of low levels of expression but a staining pattern suggesting an ER localization for Bed1 was obtained when the tagged protein was overexpressed. We showed however that the behavior of Bed1 in the fractionation procedure we used was not affected by overexpression from the constitutive GAP promoter. Taken together, these two different approaches suggested that Bed1 is an integral type II membrane protein of the ER.

We discovered recently that the *BED1* gene was independently cloned as *SLC2* (Karpova et al., 1995). *slc2* mutants were identified during a screen designed to identify mutations synthetically lethal with a disruption of *CAP2*, a gene involved in actin cytoskeleton organization (Karpova et al., 1993). The phenotype associated with the *slc2-107* is different from that described here: the actin cytoskeleton is disorganized in a strain carrying the *slc2-107* allele and this strain is thermosensitive while *bed1::URA3* cells have a normal pattern of actin polarization and are not temperature sensitive (at least up to 37°C; not shown). This could be explained either by strain background differences or by the fact that the *slc2-107* mutation is semidominant, suggesting that this mutation might be associated with a gain-of-function. More recently, the sequence of the *BED1* gene appeared twice in the Genbank database: it was detected during the sequencing of chromosome IV and *BED1* is identical to *MNN10* (accession number l42540). *mnn* mutants were isolated as mutants that have aberrant carbohydrate structures in the cell wall; most of the gene products are thought to be involved in mannosylation of proteins but some could be involved in more general functions of the secretory pathway that might affect mannosylation indirectly (for review see Hercovics and Orlean, 1993). This latter hypothesis is consistent with our results.

BED1 was found to be similar to 4 ORFs in *S. pombe*, *gma12*$^+$, and 2 of its homologues and a previously unidentified ORF we called spORF. The homology between Bed1 and gma12p/cds11/cds13 was particularly significant over 4 regions in the luminal portion of these proteins (~30% identity and 65% similarity). The gma12p protein has been shown to be an α-1,2-galactosyltransferase (Chappell et al., 1994). Several galactosyltransferase activities have been detected in *S. pombe* (Chappell et al., 1994; Ballou and Ballou, 1995) and the *gma12*$^+$ gene belongs to a large family of related genes in *S. pombe* (Chappell, T., personal communication). Although the structures of the two proteins are clearly similar, Bed1 has a larger cytoplasmic domain. On the other hand, this domain is comparable in size with the corresponding domain of spORF and, furthermore, comparison of the available sequences of spORF and Bed1 (see Fig. 7) showed that the degree of similarity between Bed1 and spORF was higher than between Bed1 and gma12p (~40–50% identity and 70% similarity). We conclude from these observations that spORF is more likely than gma12$^+$ to be the homologue of BED1 in *S. pombe*. Indeed, gma12$^+$ could not complement the morphological defects observed in bed1 cells, although it was shown to be enzymatically active in vitro in extracts from *S. cerevisiae* cells overexpressing gma12p under the control of the GAL1 promoter (not shown). Moreover, localization of gma12p in the Golgi apparatus (Chappell et al., 1994) is distinct from that of Bed1. Finally, gma12p is involved in bulk modification of proteins of the cell wall, a phenomenon particular to *S. pombe*, that has not been detected in *S. cerevisiae*; we propose that the role of Bed1 is more specific (see below).

It was surprising to find homology between Bed1 and a galactosyltransferase since, to our knowledge, no galactosyl modifications have been described for glycoproteins or glycolipids in *S. cerevisiae*. We were unable to detect any galactosyltransferase activity in extracts from wild-type cells or from cells overexpressing Bed1 under conditions where ectopically overexpressed gma12p showed significant activity (not shown). This assay, based on conditions described for gma12p (Chappell and Warren, 1992), is somewhat restrictive and does not rule out the possibility that *Bed1* could be a galactosyltransferase that cannot use α-methylmannoside or α-methylgalactoside as an acceptor. Furthermore, the idea that Bed1 is a galactosyltransferase is in conflict with the fact that no phenotype has been described in association with disruption of the *GAL10* gene encoding UDP-glucose 4-epimerase, the enzyme responsible for interconversion of UDP-glucose and UDP-galactose. We verified that the disruption of this gene in our genetic background did not confer a morphological phenotype similar to that of *bed1::URA3* cells when grown on glucose medium (not shown). An alternative possibility is that another epimerase is present in *S. cerevisiae* and is responsible for the production of UDP-galactose from UDP-glucose for the purpose of galactosyl modification of specific proteins or lipids. Such modification targeted to specific protein or lipid species could have escaped detection in analysis of bulk glycoproteins or glycolipids. This raises the intriguing possibility that specific galactosyl modification may be involved in signaling the isotropic to polarized switch in secretion. We are currently investigating using a PCR approach the hypothesis that *S. cerevisiae* contains other glucose-4-epimerase(s). Alternatively, Bed1 may catalyze a different glycosyl modification although, based on precedent, this is unlikely: high levels of structural homology have been detected only between enzymes that catalyze analogous glycosylation reactions (Kleene and Berger, 1993).

A simple model to explain the role of Bed1 in polarized growth and therefore in bud emergence is that Bed1 is involved in modification of an effector protein that controls the targeting of the secretory vesicles via the actin cytoskeleton in the context of the switch from isotropic to polarized growth at the G1/S phase boundary. In an alternative model, Bed1 might catalyze a modification that leads to local reorganization of the membrane and/or the cell wall at the bud site, allowing vesicles to fuse more efficiently with the plasma membrane. Elucidation of the function of Bed1 will require the identification and characterization of its target(s).

It is interesting that *bed1* mutant cells show defects in polarized secretion and that cell division occurs when buds are unusually small (Fig. 4). One interpretation of this ob-

servation is that bud emergence, albeit with a delay, can be initiated without highly polarized secretion but that, under such circumstances, significant growth cannot occur until a bud becomes an autonomous cell. Thus, whereas bud growth is normally integrated as a phase of each cell cycle, in *bed1* cells, it may be pushed forward to the subsequent cell cycle.

In summary, we have characterized a new gene that is required for efficient bud emergence and apical growth. Cells carrying a disrupted allele of *BED1* are viable but depend upon a morphogenesis checkpoint to survive. The defects observed in *bed1* cells indicate that this protein is in a pathway downstream or parallel to the actin polarization pathway in mediating the switch from isotropic to polarized growth. The fact that Bed1 shares significant homology with an *S. pombe* galactosyltransferase suggests that glycosylation might have an important signaling role in this process.

We thank Fred Cross, Mark Johnston, Dave Stuart, Martin Snider, and Henar Valdivieso for generous gift of plasmids and Mark Rose for the anti-Kar2 serum; George Klier for help with the confocal microscopy; Tom Chappell, John Cooper, and Martin Snider for sharing results before publication. Danny Lew, Dave Stuart, and Curt Wittenberg are acknowledged for the critical reading of this manuscript. G. Mondésert would like to thank the members of the Reed, Wittenberg, and Russell Laboratories for fruitful interactions, especially Marie-Noëlle Simon and Eric Bailly for daily discussions and encouragement and Danny Lew for discussions on morphogenesis.

G. Mondésert acknowledges fellowships from the European Molecular Biology Organization and the Human Frontiers in Science Program. This research was supported by a U.S. Public Health Service Grant (GM38328) to S. I. Reed.

Received for publication 23 June 1995 and in revised form 17 October 1995.

References

Adams, A. E. M., and J. R. Pringle. 1984. Relationship of actin and tubulin distribution to bud growth in wild-type and morphogenetic-mutant *Saccharomyces cerevisiae*. *J. Cell Biol.* 98:934–945.

Adams, A. E. M., and J. R. Pringle. 1990. Staining of actin with fluorochrome-conjugated phalloidin. *Methods Enzymol.* 194:729–732.

Altschul, S. F., W. Gish, W. Miller, E. W. Myers, and D. J. Lipman. 1990. Basic local alignment search tool. *J. Mol. Biol.* 215:403–410.

Amon, A., S. Irniger, and K. Nasmyth. 1994. Closing the cell cycle circle in yeast: G2 cyclin proteolysis initiated at mitosis persists until the activation of G1 cyclins in the next cycle. *Cell.* 77:1037–1050.

Ballou, L., and C. Ballou. 1995. *Schizosaccharomyces pombe* mutants that are defective in glycoprotein galactosylation. *Proc. Natl. Acad. Sci. USA.* 92: 2790–2794.

Bretscher, A., B. Drees, E. Harsay, D. Schott, and T. Wang. 1994. What are the basic functions of microfilaments? Insights from studies in budding yeast. *J. Cell Biol.* 126:821–825.

Chant, J. 1994. Cell polarity in yeast. *Trends Genet.* 10:328–333.

Chappell, T., and G.Warren. 1992. Galactosyltransferase from the fission yeast *Schizosaccharomyces pombe*. *J. Cell Biol.* 109:2693–2702.

Chappell, T., N. Hajibagheri, K. Ayscough, M. Pierce, and G. Warren. 1994. Localization of an α-1,2-galactosyltransferase activity to the Golgi apparatus of *Schizosaccharomyces pombe*. *Mol. Biol. Cell.* 5:519–528.

Donnelly, S. F., M. J. Pocklington, D. Pallota, and E. Orr. 1993. A proline rich protein, verprolin, involved in cytoskeletal organization and cellular growth in the yeast *Saccharomyces cerevisiae*. *J. Mol. Microbiol.* 10:585–596.

Elble, R. 1992. A simple and efficient procedure for transformation of yeasts. *Biotechniques.* 13:18–20.

Ghiara, J. B., H. E. Richardson, K. Sugimoto, M. Henze, D. J. Lew, C. Wittenberg, and S. I. Reed. 1991. A cyclin B homologue in *S. cerevisiae:* chronic activation of the Cdc28 protein kinase by cyclin prevents exit from mitosis. *Cell.* 65:163–174.

Graham, T. R., M. Seeger, G. S. Payne, V. L. MacKay, and S. D. Emr. 1994. Clathrin-dependent localization of α 1,3 mannosyltransferase to the Golgi complex of *Saccharomyces cerevisiae*. *J. Cell Biol.* 127:667–678.

Grandin, N., and S. I. Reed. 1993. Differential function and expression of *S. cerevisiae* B-type cyclins in mitosis and meiosis. *Mol. Cell. Biol.* 13:2113–2125.

Hercovics, A., and P. Orlean. 1993. Glycoproteins biosynthesis in yeast. *FASEB (Fed. Am. Soc. Exp. Biol.) J.* 7:540–550.

High, S., and B. Dobberstein. 1992. Mechanisms that determine the transmembrane disposition of proteins. *Curr. Opin. Cell. Biol.* 4:581–586.

Hinnebusch, A. G., and S. W. Liebman. 1991. Protein synthesis and translational control in *Saccharomyces cerevisiae*. *In* The Molecular Biology of the Yeast *Saccharomyces*: Genome Dynamics, Protein Synthesis and Energetics. Cold Spring Harbor Laboratory Press, Cold Spring Harbor, New York. 1: 627–735.

Karpova, T. S., M. M. Lepetit, and J. A. Cooper. 1993. Mutations that enhance the *cap2* null mutant phenotype in *Saccharomyces cerevisiae* affect the actin cytoskeleton, morphogenesis and pattern of growth. *Genetics.* 135:693–709.

Karpova, T. S., K. Tatchell, and J. A. Cooper. 1995. Actin filaments in yeast are unstable in the absence of capping protein or fimbrin. *J. Cell Biol.* In press.

Kilmartin, J. V., and A. E. M. Adams. 1984. Structural rearrangements of tubulin and actin during the cell cycle of the yeast *Saccharomyces*. *J. Cell Biol.* 98: 922–933.

Kleene, R., and E. G. Berger. 1993. The molecular and cell biology of glycosyltransferases. *Biochim. Biophys. Acta.* 1154:283–325.

Lew, D. J., and S. I. Reed. 1993. Morphogenesis in the yeast cell cycle: regulation by Cdc28 and cyclins. *J. Cell Biol.* 120:1305–1320.

Lew, D. J., and S. I. Reed. 1995*a*. A cell cycle checkpoint monitors cell morphogenesis in budding yeast. *J. Cell Biol.* 129:739–749.

Lew, D. J., and S. I. Reed. 1995*b*. Cell cycle control of morphogenesis in budding yeast. *Curr. Opin. Genet. Dev.* 5:17–23.

Lew, D. J., N. J. Marini, and S. I. Reed. 1992. Different G1 cyclins control the timing of cell cycle commitment in mother and daughter cells in the budding yeast *Saccharomyces cerevisiae*. *Cell.* 69:317–327.

Mulholland, J., D. Preuss, A. Moon, A. Wong, D. Drubin, and D. Botstein. 1994. Ultrastructure of the yeast actin cytoskeleton and its association with the plasma membrane. *J. Cell Biol.* 125:381–391.

Nasmyth, K. 1993. Control of the yeast cell cycle by the *Cdc28* protein kinase. *Curr. Opin. Cell Biol.* 5:166–179.

Preuss, D., J. Mulholland, A. Franzusoff, N. Segev, and D. Botstein. 1992. Characterization of the *Saccharomyces* Golgi complex through the cell cycle by immunoelectron microscopy. *Mol. Biol. Cell.* 3:789–803.

Pringle, J. R. 1991. Staining of bud scars and other cell wall chitin with calcofluor. *Methods Enzymol.* 194:732–735.

Pringle, J. R., A. E. M. Adams, D. G. Drubin, and B. K. Haarer. 1991. Immunofluorescence methods for yeast. *Methods Enzymol.* 194:565–602.

Reed, S. I. 1992. The role of p34 kinases in the G1 to S-phase transition. *Annu. Rev. Cell Biol.* 8:529–561.

Richardson, H. E., C. Wittenberg, F. R. Cross, and S. I. Reed. 1989. An essential G1 function for cyclin-like proteins in yeast. *Cell.* 59:1127–1133.

Rose, M. D., P. Novick, J. H. Thomas, D. Botstein, and G. R. Fink. 1987. A *Saccharomyces cerevisiae* genomic plasmid bank based on a centromere-containing shuttle vector. *Gene (Amst.).* 60:237–243.

Sherman, F., G. Fink, and J. B. Hicks. 1982. Methods in Yeast Genetics. Cold Spring Harbor Laboratory, Cold Spring Harbor, New York.

Sikorski, R. S., and P. Hieter. 1989. A system of shuttle vectors and yeast host strains designed for efficient manipulation of DNA in *Saccharomyces cerevisiae*. *Genetics.* 122:19–27.

Stueland, C. S., D. J. Lew, and S. I. Reed. 1993. Full activation of p34*CDC28* histone H1 kinase activity is unable to promote entry into mitosis in checkpoint-arrested cells of the yeast *Saccharomyces cerevisiae*. *Mol. Cell. Biol.* 13:3744–3755.

Tyers, M., G. Tokiwa, R. Nash, and B. Futcher. 1992. The Cln3-Cdc28 kinase complex of *S.cerevisiae* is regulated by proteolysis and phosphorylation. *EMBO (Eur. Mol. Biol. Organ.) J.* 11:1773–1784.

Van der Leij, I., M. M. Franse, Y. Ergelsma, B. Distel, and H. F. Tabak. 1994. *PAS10* is a tetratricopeptide-repeat protein that is essential for the import of most matrix proteins into peroxisomes of *Saccharomyces cerevisiae*. *Proc. Natl. Acad. Sci. USA.* 90:11782–11786.